Electronic Supplementary Material (ESI) for Soft Matter.

Scale-Invariance in Miniature Coarse-Grained Red Blood Cells by Fluctuation Analysis: Supporting Information

PAUL APPSHAW, ANNELA M. SEDDON, AND SIMON HANNA

1. YUAN POTENTIAL

To model the lipid bilayer membrane this work implements the orientation dependant lipid-lipid interaction potential $U(\mathbf{r}_{ij},\mathbf{n}_i,\mathbf{n}_j)$ developed by Yuan et al. [1]. In this model, the lipid bilayer is modelled as a one-particle-thick monolayer of CG particles, each representing a collection of lipids and having five degrees of freedom: three translational and two rotational. The separation of two such pseudo-particles i and j is given by $r = |\mathbf{r}_{ij}| = |\mathbf{r}_i - \mathbf{r}_j|$ and their relative orientations by normal vectors $\mathbf{n}$, where rotation about $\mathbf{n}$ is not considered (see Figure S1).

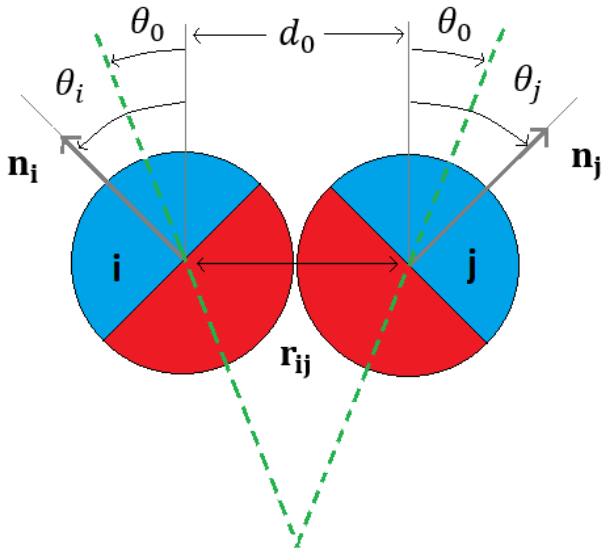

Fig. S1. Schematic expressing the angular components of two interacting CG lipids, at positions $\{\mathbf{r}_i,\mathbf{r}_j\}$, and separation $\mathbf{r}_{ij}$. Each particle is axisymmetric with a unit vector $\{\mathbf{n}_i,\mathbf{n}_j\}$ fixed to them, representing the axis of symmetry. The angular parameters $\{\theta_i,\theta_j\}$ are dependant on these normal vectors. The orientation of each particle is indicated by the colour of their halves.

The Yuan potential is dependant on two functions, $u(r)$ and $\phi(\hat{\mathbf{r}}_{ij},\mathbf{n}_i,\mathbf{n}_j)$, characterising the translational and angular dependencies respectively. The function ϕ acts to weight the interaction strength between two CG lipid particles according to their relative orientation, and is given by

$$\phi(\hat{\mathbf{r}}_{ij},\mathbf{n}_i,\mathbf{n}_j) = 1 + \mu_Y[a(\hat{\mathbf{r}}_{ij},\mathbf{n}_i,\mathbf{n}_j) - 1] \tag{S1}$$

$$a(\hat{\mathbf{r}}_{ij},\mathbf{n}_i,\mathbf{n}_j) = (\mathbf{n}_i \times \hat{\mathbf{r}}_{ij}) \cdot (\mathbf{n}_j \times \hat{\mathbf{r}}_{ij}) + \sin\theta_0 (\mathbf{n}_i - \mathbf{n}_j) \cdot \hat{\mathbf{r}}_{ij} - \sin^2\theta_0, \tag{S2}$$

where $\hat{\mathbf{r}}_{ij} = \mathbf{r}_{ij}/r$, and θ_0 and μ_Y are parameters characteristic to the model. θ_0 corresponds to the most energetically favourable angular configuration of particles - that when $\theta_i = \theta_j = \theta_0$ - thus links to the

membranes spontaneous curvature c_0, approximated by

$$c_0 \sim \frac{2}{d_0} \sin\theta_0, \tag{S3}$$

where d_0 is the average interparticle separation. μ_Y weights the energy penalty for deviation away from θ_0, thus relates to the membranes bending rigidity.

To provide the intermediate fluid phase necessary to produce the correct diffusion behaviour, a two branch function is adopted [1]. The position function separates attractive and repulsive branches as

$$u(r) = \begin{cases} u_R(r) = \varepsilon \left[\left(\frac{r_{\min}}{r}\right)^4 - 2\left(\frac{r_{\min}}{r}\right)^2 \right], & r < r_{\min} \\ u_A(r) = -\varepsilon \cos^{2\zeta}\left(\frac{\pi}{2}\frac{r-r_{\min}}{r_c-r_{\min}}\right), & r_{\min} < r < r_c \end{cases} \tag{S4}$$

with energy unit $\varepsilon = \sigma_\varepsilon$ defining the energy well, and distance $r_{\min}$ being that which minimises the potential energy. As in the 12-6 LJ, $r_{\min} = \sqrt[6]{2}\sigma$, in length unit $\sigma = \sigma_r$. The cutoff radius is given as $r_c = 2.6\sigma$, to include second neighbour interactions. The attractive branch smoothly decays to zero at r_c, with exponent ζ controlling the slope of the branch. The full anisotropic pair-potential is then given by

$$U = \begin{cases} u_R(r) + \varepsilon \left[1 - \phi(\hat{\mathbf{r}}_{ij}, \mathbf{n}_i, \mathbf{n}_j)\right], & r < r_{\min} \\ u_A(r)\phi(\hat{\mathbf{r}}_{ij}, \mathbf{n}_i, \mathbf{n}_j), & r_{\min} < r < r_c \end{cases} \tag{S5}$$

2. UNITS

To convert each variable i from non-dimensional "model" LJ units (denoted i^M) to "real" SI units (denoted i^R), dimensional conversion parameters σ_i are used. Each system quantity has conversion parameter defined as such as follows:

- Length $\sigma_r = 5$nm: Defined by the lipid bilayer thickness, being the minimum length-scale required in the system [2].
- Temperature $\sigma_T = 1.3 \times 10^2$K: Defined by $T^R = \sigma_T T^M$, assuming a room temperature system $T^R = 293$K, and with target model temperature $T^M = 0.23$ following previous application of the model [1, 3].
- Energy $\sigma_\varepsilon = 1.8 \times 10^{-20}$J: From LJ relationship $\sigma_\varepsilon = \sigma_T k_B$, where k_B is the Boltzmann constant.
- Pressure $\sigma_P = 1.4 \times 10^5 \mathrm{N/m^2}$: From LJ relationship $\sigma_P = \sigma_\varepsilon / \sigma_r^3$
- Force $\sigma_F = 3.5$pN: From LJ relationship $\sigma_F = \sigma_\varepsilon / \sigma_r$.
- Time $\sigma_t = 80$ns: Evaluated from the mean-square-displacement of a simulated patch of isolated lipid membrane, as described in the next section (A).
- Mass $\sigma_m = 4.9 \times 10^{-6}$kg: From LJ relationship $\sigma_m = \sigma_\varepsilon (\sigma_t / \sigma_r)^2$.

A. Diffusivity and Timescale

At $T_M = 0$, a RBC membrane forms a solid phase with a long-range order [4]. As temperature is then increased this order is broken as fluctuations emerge, characterising a fluid phase. The presence of such a fluid phase at $T_M = 0.23$ can be verified in the Yuan model by showing that the mean-square-displacement MSD increases linearly with time for a tensionless planar lipid membrane. The two-dimensional MSD is calculated as [5]

$$\mathrm{MSD}(t) = \frac{1}{N} \sum_{i=1}^{N} \left\langle \left(\mathbf{r}_i(t) - \mathbf{r}_i(0)\right)^2 \right\rangle, \tag{S6}$$

where $\mathbf{r}_i = (x, y)$ is the position of a particle at time t with-respect-to the centre of mass of the bilayer plane. From Einstein's equation for a two-dimensional membrane, the in-plane diffusivity is then given by

$$D = \lim_{t \to \infty} \left(\frac{\mathrm{MSD}(t)}{4t} \right). \tag{S7}$$

Simulations are performed on the two-dimensional plane of lipid bilayer, as described in section 3.2 of the main paper. Figure S2 shows the MSD and diffusivity over time, with $D = 6.7 \times 10^{-3} \sigma_r^2 / \sigma_t$ taken between 4×10^5 and 2×10^6 steps, when the membrane is deemed equilibrated. Comparing this against a typical diffusion for an RBC bilayer $D \sim 2 \times 10^{-8} \mathrm{cm^2/s}$ at 300K [6], the timescale is found to be $\sigma_t = 80$ns. This is comparable to past implementation of the model, with Fu et al. determining $\sigma_t = 100$ns [3].

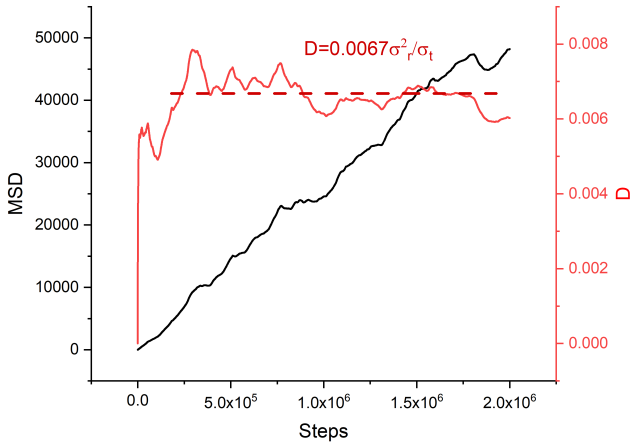

Fig. S2. MSD (black) and two-dimensional diffusivity (red) against time for the lipid bilayer patch. Membrane configurations are taken every 1000 steps, and discarded if the surface tension is calculated to be greater than $\pm 0.01\sigma_F/\sigma_r$ offset from zero.

3. BENCHMARK

To evaluate the feasibility of the model for whole-cell simulations at full physical size $D^M = D^M_{RBC} = 1600$ ($D^R = 8\mu$m), timings are compared for varying particle numbers and type proportionalities. The base system tested is that for the shape evolution over 290,000 steps, but excluding the compression phase for consistency between cell sizes. To first determine the scalability of the model, whole-cell systems are timed for varying cell size D^M, thus total number of particles (see Figure S3A). The proportion of water-to-membrane particles is kept consistent with D^M, with a constant proportion of super-cell volume containing membrane. Unfortunately, the LAMMPS deployed model is found to scale poorly with number of nodes. Only at $D^M \geq 150$ does an increased number of nodes start to show any improvement. Continuation of the exponential trend would expect simulation of a $D^M = 1600$ cell to take around 2000 years to complete on 4 nodes.

To then compare the contributing load from the complex Yuan membrane mechanics against the simple LJ fluid, systems are tested with varying ratios of water-to-lipid particles (see Figure S3B). Linear regression finds that the water particles account for only 9% of the total simulation time relative to the membrane particles. This indicates an explicit solvent to only marginally constrain feasible simulation scales. Furthermore, the implication is that it is then the implementation of the custom Yuan pair potential function that is primarily responsible for the poor scalability of the model.

4. FLUCTUATION ANALYSIS

To analyse the rigidity in the whole cell, fluctuation analysis can be applied to a three-dimensional vesicle by measuring the thermal undulations of the membrane over time. To achieve this, many sequential contours of the membrane are taken - two-dimensional slices of the cell surface. The analysis technique is applied here following the methodology developed successively by Faucon et al. [7], Mitov et al. [8], and Melerard et al. [9].

The positional vector of a point on the membrane at time t is defined in spherical coordinates by $\mathbf{r}(\theta,\phi,t) = R_0[1+u(\theta,\phi,t)]\mathbf{e}_r(\theta,\phi)$, with unit normal vector $\mathbf{e}_r(\theta,\phi)$. The displacement-field $u(\theta,\phi,t)$ represents the local deviation from a perfectly spherical surface of radius R_0; the amplitude of fluctuation in the direction (θ,ϕ). As an RBC is not spherical, R_0 is chosen as the radius of a perfect sphere of equivalent volume $R_0 = (3V_0/4\pi)^{1/3}$. The vesicle shape $u(\theta,\phi,t)$ is decomposed into the sum of a static average value $u_0(\theta,\phi)$ and dynamic perturbation $\delta u(\theta,\phi,t)$, where $\langle u(\theta,\phi,t)\rangle = u_0(\theta,\phi)$ and $\langle \delta u(\theta,\phi,t)\rangle = 0$.

The dynamic shape perturbations can be expressed in the spherical harmonics basis as

$$\delta u(\theta,\phi,t) = \sum_{n=0}^{n=n_{max}} \sum_{m=-n}^{m=n} U_n^m(t) Y_n^m(\theta,\phi), \tag{S8}$$

with spherical harmonics functions $Y_n^m(\theta,\phi)$, and time-dependent membrane displacements $U_n^m(t)$. The

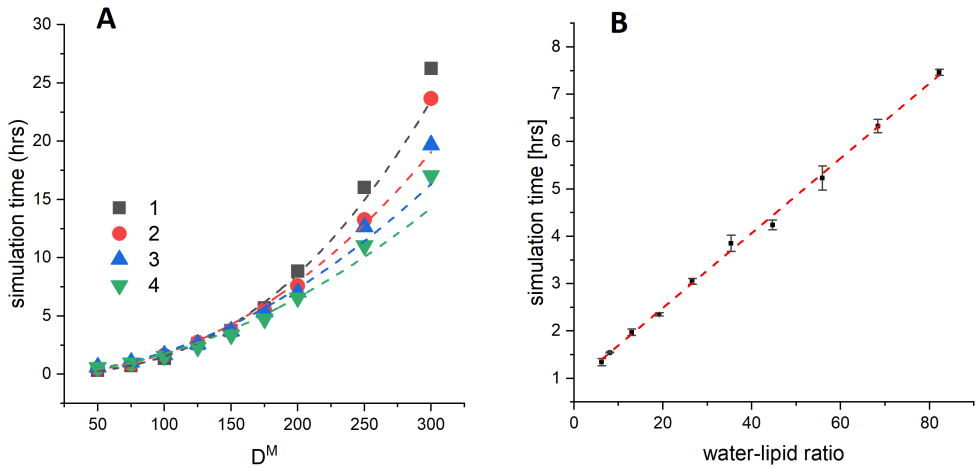

Fig. S3. (**A**) Plot of simulation time against cell-size-associated volume when run on 1-4 28-core nodes. (**B**) Plot of simulation time for systems comprised of varying proportions of water to membrane particles. Standard error in plot **B** is obtained from repeating each simulation 3 times.

upper modes are capped at a value $n_{max} = \sqrt{N}$, being the root of the number of membrane lipids [**?**]. We only observe the equatorial cross-section of the vesicle (taking fixed polar angle $\theta = \pi/2$), so can omit the m order of decomposition.

Assuming that the fluctuations remain small ($u(\theta,\phi,t) \ll 1$), the mean square amplitudes of membrane fluctuations can be derived to be

$$\left\langle |U_n^m(t)|^2 \right\rangle = \frac{k_B T}{B} \frac{1}{(n-1)(n+2)[\bar{\Sigma}+n(n+1)]}, \; n \geq 2, \; \bar{\Sigma} \geq -6 \tag{S9}$$

with reduced membrane tension $\bar{\Sigma} = \sigma R^2/B$ [**?**]. The case $n = 0$ corresponds to variation in the mean vesicle radius, and $n = 1$ to variation in the centre of mass. Neither of these are relevant for the fluctuation analysis, so only modes $n \geq 2$ are considered. $\bar{\Sigma}$ is constrained above -6, so as to keep the denominator of Eq. S9 from going negative. As $\bar{\Sigma}$ measures the tension in the vesicle, it also dictates the maximum amplitude of fluctuations, by being a measure of the excess area in the membrane. As $\bar{\Sigma} \to \infty$ the membrane is increasingly tightly spherical, with undulations becoming too small to measure. Conversely, as $\bar{\Sigma} \to -6$ the fluctuations are possibly very large, degrading the statistics of the low mode numbers.

To establish a connection between the experimentally observable two-dimensional contour slices and three-dimensional model that lead to Eq. S9, the angular auto-correlation function (ACF) is introduced. For a given contour, the angular ACF is given by

$$\xi(\gamma,t) = \frac{1}{2\pi R_0^2} \int_{\phi=0}^{2\pi} [\rho(\phi+\gamma,t) - \rho(t)]\,[\rho^*(\phi,t) - \rho(t)]\,\mathrm{d}\phi \tag{S10}$$

with angle about the contour γ, radius at a point on the contour $\rho(\phi,t) = \mathbf{r}(\pi/2,\phi,t)$ and the ϕ-mean radius of a single contour $\rho(t) = \langle \rho(\phi,t) \rangle$ [9]. The temporal mean of the ACF can be expanded using Legendre polynomials as [**?**]

$$\langle \xi(\gamma,t) \rangle = \xi(\gamma) = \sum_{n=2}^{n_{max}} \langle B_n(t) \rangle P_n(\cos\gamma), \tag{S11}$$

with coefficients $\langle B_n(t) \rangle$. These coefficients are defined as the time-average amplitudes of decomposition of the ACF in the Legendre polynomial basis, and relate to $\left\langle |U_n^m(t)|^2 \right\rangle$ by

$$\langle B_n(t) \rangle = \frac{2n+1}{4\pi} \left\langle |U_n^m(t)|^2 \right\rangle. \tag{S12}$$

From the expression of the ACF as a Legendre polynomial series in Eq. S11, the coefficients B_n can be calculated from the experimentally obtainable ACF data as [10]

$$B_n(t) = \left(\frac{2n+1}{2} \right) \int_0^\pi \sin(\gamma) \xi(\gamma,t) P_n(\cos\gamma) \mathrm{d}\gamma. \tag{S13}$$

By calculating the coefficients $B_n(t)$ averaged over many contour configurations, the constants B and $\bar{\Sigma}$ can be determined by a χ^2 fit of $\langle B_n(t)\rangle$ against n through Eq. S12 and Eq. S9.

The procedure is thus employed in our simulations as follows:

1. Contours are taken in the (x,y) plane of the cell, being that around the circular outer ring of the biconcave cell membrane. Each angular point $\rho = (\phi,t)$ of the contour is simply defined by the lipid particle within that segment having the largest radius from the contour midpoint.

2. The angular ACF can then be approximated as

$$\xi(j,t) = \frac{1}{2\pi R_0^2} \sum_{i=0}^{i=N_\phi} [\rho(i+j,t) - \rho(t)] \cdot [\rho(i,t) - \rho(t)] \Delta j \tag{S14}$$

   for each angular step j of size $\Delta j \equiv \Delta i$ around the contour, in the range $0 \leq j < N_\phi/2$.

3. Eq. S13 is converted into a sum over j as

$$B_n(t) = \frac{2n+1}{2} \sum_{j=0}^{j=N_\phi/2} \xi(j,t) \sin(j) P_n(\cos j) \Delta j \tag{S15}$$

   with the mean $\langle B_n(t)\rangle$ then taken over many consecutive contour configurations.

4. The calculated mean coefficients are finally plotted against n, with a χ^2 fit determining the two constants B and $\bar{\Sigma}$.

Resulting graphs for the fits of Eq. S12 to the mean-squared-coefficients are given in Figure S4 for those cell sizes not shown in the main paper.

REFERENCES

1. H. Yuan, C. Huang, J. Li, G. Lykotrafitis, and S. Zhang, "One-particle-thick, solvent-free, coarse-grained model for biological and biomimetic fluid membranes," Phys. Rev. E **82**, 011905 (2010).
2. H. Yuan, C. Huang, and S. Zhang, "Dynamic shape transformations of fluid vesicles," Soft Matter **6**, 4571–4579 (2010).
3. S.-P. Fu, Z. Peng, H. Yuan, R. Kfoury, and Y.-N. Young, "Lennard-jones type pair-potential method for coarse-grained lipid bilayer membrane simulations in lammps," Comput. Phys. Commun. **210**, 193–203 (2017).
4. H. Li and G. Lykotrafitis, "Two-component coarse-grained molecular-dynamics model for the human erythrocyte membrane," Biophys. J. **102**, 75–84 (2012).
5. H. Li and G. Lykotrafitis, "Erythrocyte membrane model with explicit description of the lipid bilayer and the spectrin network," Biophys. J. **107**, 642–653 (2014).
6. J. A. Bloom and W. W. Webb, "Lipid diffusibility in the intact erythrocyte membrane," Biophys. J. **42**, 295–305 (1983).
7. J. Faucon, M. D. Mitov, P. Méléard, I. Bivas, and P. Bothorel, "Bending elasticity and thermal fluctuations of lipid membranes: Theoretical and experimental requirements," J. Phys. **50**, 2389–2414 (1989).
8. M. D. Mitov, J. F. Faucon, P. Méléard, I. Bivas, and P. Bothorel, "Thermal fluctuations of membranes," in *Advances in Supramolecular Chemistry Vol. 2,* G. W. Gokel, ed. (Jai Press, Greenwich, 1992), pp. 93–139.
9. P. Méléard, T. Pott, H. Bouvrais, and J. H. Ipsen, "Advantages of statistical analysis of giant vesicle flickering for bending elasticity measurements," Eur. Phys. J. E **34**, 116 (2011).
10. J. Henriksen, A. C. Rowat, and J. H. Ipsen, "Vesicle fluctuation analysis of the effects of sterols on membrane bending rigidity," Eur. Biophys. **33**, 732–741 (2004).

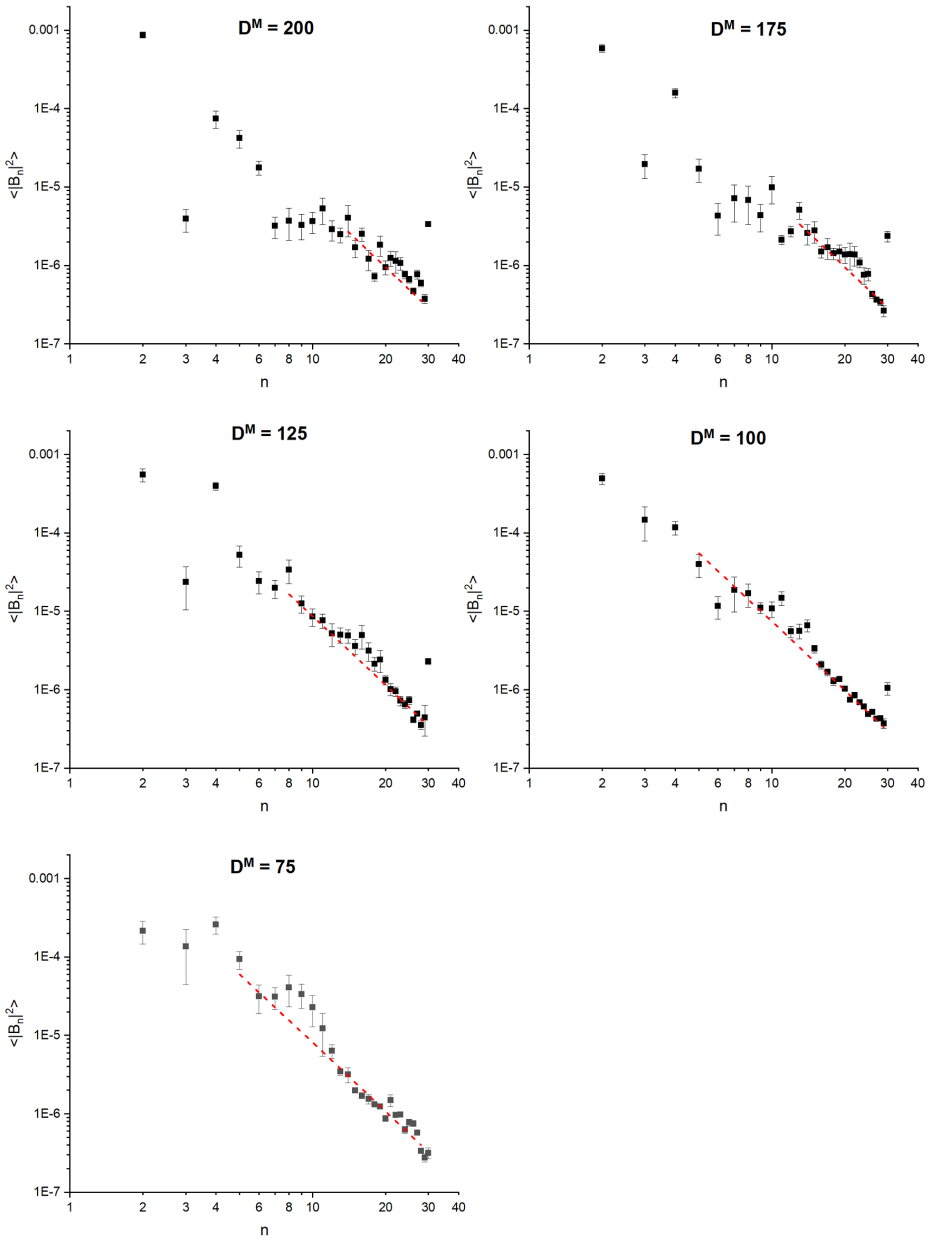

Fig. S4. Graphs of the spectra of coefficients for each cell size not shown in the main paper. Coefficients are taken from the mean result of 1000 contours from 6 different cells.